

EFFECTS OF THE AMOUNT OF STARCH AND THE HOLDING TIME ON THE SYNTHESIS OF SiC–TiC COMPOSITE POWDERS

[#]JILIN HU, YU CAO, XIN LIU, LING ZHU, JING LI, JIN WEN, YANGXI PENG, ZHANJUN CHEN

Hunan Provincial Key Laboratory of Fine Ceramics and Powder Materials, School of Materials and Environmental Engineering, Hunan University of Humanities, Science and Technology, Loudi 417000, China

[#]E-mail: hujilin@126.com

Submitted September 3, 2021; accepted October 22, 2021

Keywords: Influence, Carbothermal reduction method, Silicon carbide, Titanium carbide, Preparation

SiC–TiC composite powders were synthesised through carbothermal reduction under an argon atmosphere by using silica sol, starch, and TiO₂ as the raw materials. The influences of the starch dosage and holding time on the synthesis of SiC–TiC composite powder are discussed in detail. The samples were characterised using an X-ray diffractometer (XRD), an integrated thermal analyser (TG–DTA), a scanning electron microscope (SEM), and an energy spectrometer (EDS). The results showed that the SiC–TiC composite powders were completely synthesised after holding at 1550 °C for 3 h when the amount of excess starch was 5 wt. % and after holding at 1550 °C for 2 h when the amount of excess starch was 10 - 20 wt. %. The morphological characteristics of the powder samples with 5 - 15 wt. % excess starch calcined at 1550 °C for 2 h were mainly flake particles, spherical particles, irregularly shaped particles and elongated whiskers. Conversely, no whiskers were found in the powder samples calcined at 1550 °C for 2 h when the amount of excess starch was 20 wt. %.

INTRODUCTION

Silicon carbide (SiC) has a series of advantages, such as high-temperature strength, high hardness, high thermal conductivity, good chemical stability, and excellent oxidation resistance. It is widely used in many fields, such as the chemical industry, the textile industry, in machinery, the military industry, and in energy, and its application prospects vary broadly [1-3]. Nevertheless, the room-temperature strength and fracture toughness of SiC are low, thereby limiting its application range [4]. Titanium carbide (TiC) is an important engineering material, with a high hardness (28 - 33 GPa), high melting point (> 3000 °C), good chemical stability, high electrical and thermal conductivities, high fracture toughness, and other excellent comprehensive performance parameters [5-7]. As such, a SiC and TiC composite can achieve the complementarity of the properties of the two materials, resulting in the enhanced performance of the SiC–TiC composite, which can be applied to more fields [8]. SiC–TiC ceramic powders prepared by direct mechanical mixing have inhomogeneity in a mixed powder composition, which affects the microstructure and related properties of the SiC–TiC composites to a certain extent. Therefore, high-quality SiC–TiC ultrafine composite powders should be prepared with small particles, uniform mixing, and good dispersibility to meet material performance requirements.

Ultrafine carbide powders are commonly prepared using various methods, including carbothermal reduction [9-10], mechanical alloying [11], chemical vapour

deposition [12], and combustion synthesis [13]. Carbothermal reduction is currently the most important preparation method used in industrial production because of its low-cost raw materials, simple preparation, and easy realisation of a uniform compound of powders. In our previous research, SiC–TiC ultrafine composite powders were prepared through carbothermal reduction by selecting inorganic carbon sources, such as carbon black [14] and graphite [15]. As an organic carbon source, starch easily forms fine carbon particles during high-temperature carbonisation and decomposition in an argon atmosphere, which is conducive to the generation of an ultrafine carbide powder [16]. In other previous work [15], starch was chosen as the raw carbon source material, and the influence of different reaction temperatures on the phase composition, particle size distribution, and microstructure of SiC–TiC composite powders was discussed. In the present study, we intend to focus on the effects of the amount of starch and the holding time on the phase composition and microstructure of SiC–TiC composite powders synthesised using starch as a carbon source.

EXPERIMENTAL

Processing

Silica sol (SiO₂, 28 wt. %, Hunan Changsha Water Glass Factory, Changsha, China), soluble starch ((C₆H₁₀O₅)_n, purity of ≥ 99.0 %, Hunan Xiangzhong Chemical Reagent Co., Ltd., Loudi, China), and TiO₂

(purity of $\geq 99.0\%$, $D_{50} = 1.70\ \mu\text{m}$, Shantou Guanghua Chemical Co., Ltd., Shantou, China) were used as the starting materials for the synthesis of the SiC–TiC composite powders. The preparation of the SiC–TiC composite powders is shown in Figure 1. The amounts of silica sol, starch, and TiO_2 were adjusted to yield a TiC/SiC molar ratio of 7:3. The amounts of starch were designed to be in excess of 5 wt. %, 10 wt. %, 15 wt. %, and 20 wt. % of the theoretical calculation. These raw materials were uniformly mixed in a planetary ball mill at a speed of $400\ \text{rev}\cdot\text{min}^{-1}$ for 2 h by using SiC balls as the grinding body and anhydrous ethanol as the dispersing medium (the solid-to-liquid mass ratio was set to 1:2). The well-mixed starting materials were taken out and dried at $80\ ^\circ\text{C}$ for 24 h. After being ground, they were placed in a graphite crucible and in a high-temperature tubular electric furnace. The high-temperature synthesis reaction was carried out from room temperature to $1550\ ^\circ\text{C}$ at a heating rate of $10\ ^\circ\text{C}\cdot\text{min}^{-1}$ in an argon atmosphere. The holding times at the desired temperature were 1, 2, and 3 h. Subsequently, the furnace was cooled naturally to room temperature, and the SiC–TiC composite powders were obtained.

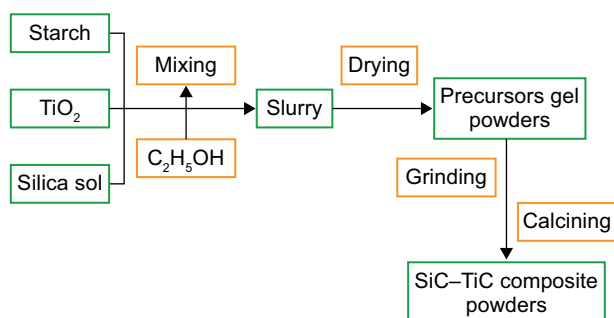


Figure 1. Preparation of the SiC–TiC composite powders.

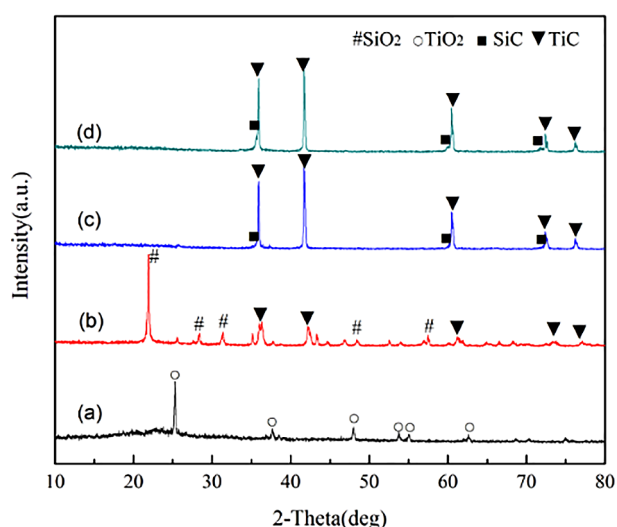


Figure 2. XRD patterns of the samples containing 5 wt. % excess of starch, dried at $80\ ^\circ\text{C}$, and maintained at $1550\ ^\circ\text{C}$ for different periods: a) $80\ ^\circ\text{C}$, b) $1550\ ^\circ\text{C} + 1\ \text{h}$, c) $1550\ ^\circ\text{C} + 2\ \text{h}$, d) $1550\ ^\circ\text{C} + 3\ \text{h}$.

Characterisation

The TG–DTA curve of a single starch was examined using a DTA-50 comprehensive thermal analyser (TG–DTA, DTA-50, Shimadzu Company, Japan). The masses of the samples before and after calcination were weighed with an electronic analytical balance (accurate to $0.1\ \text{mg}$), and the mass loss was calculated to evaluate the degree of the high-temperature synthesis. The phase composition of the powder samples dried at $80\ ^\circ\text{C}$ and calcined at $1550\ ^\circ\text{C}$ for different periods was analysed using an X-ray diffractometer (XRD, Y2000, Tongda Company, China). The morphological characteristics of the samples dried at $80\ ^\circ\text{C}$ and calcined at $1550\ ^\circ\text{C}$ for different periods were observed under a scanning electron microscope (SEM, Zeiss Sigma 500, Germany).

RESULTS AND DISCUSSION

Phase composition

Figure 2 shows the XRD patterns of the precursor powder dried at $80\ ^\circ\text{C}$ and the powder calcined at $1550\ ^\circ\text{C}$ for different periods with 5 wt. % excess of starch. In Figure 2a, the TiO_2 diffraction peak is mainly present in the precursor mixed powder dried at $80\ ^\circ\text{C}$, but no SiO_2 diffraction peak appears. These findings indicate that the SiO_2 component in the silica sol is mainly present as an amorphous form in the precursor. Consistent with these results, our previous study [17] demonstrated that the SiO_2 characteristic diffraction peak is still not found in the system after calcination at $1400\ ^\circ\text{C}$ for 2 h. When the holding time is for 1 h at $1550\ ^\circ\text{C}$, the diffraction peaks of TiC and SiO_2 simultaneously appear in the synthesised product, as shown in Figure 2b, but the characteristic diffraction peaks of SiC are still not evident at this time. This finding illustrates that TiC forms in the system under this condition, but the SiC formation has not yet fully started. Notably, the diffraction peak of carbon is not found in Figure 2b, indicating that the elemental carbon produced by the decomposition of the starch raw materials at a high temperature mainly exists in an amorphous form in the system. Our previous study [17] has also shown that the elemental carbon formed through the decomposition of glucose at a high temperature is amorphous. Indeed, elemental carbon as the main product of the decomposition of organic carbon sources, such as starch and glucose, at high temperatures is amorphous. When the holding time is 2 h, strong TiC diffraction peaks and relatively weak SiC diffraction peaks appear in the system, as illustrated in Figure 2c. Other impurity peaks are not obvious, indicating that the TiC synthesis is almost complete, but the SiC synthesis is not yet fully completed. After the holding time is extended to 3 h, the TiC diffraction peak in the system does not change significantly, but the intensity of the SiC diffraction peak further enhances, and the peak shape sharpens, as presented in Figure 2d. In summary, when

the amount of excess starch is 5 wt. %, the SiC–TiC composite powder is completely synthesised at 1550 °C for 3 h with starch as the carbon source. This observation is basically consistent with the analysis result of the mass loss in the subsequent synthesis.

Figure 3 shows the XRD patterns of the precursor powder dried at 80 °C and the powder calcined at 1550 °C for different times with 10 wt. % excess of starch. In Figure 3a, the TiO₂ diffraction peak is mainly present in the precursor mixed powder dried at 80 °C, but no SiO₂ diffraction peak forms. When the holding time is 1 h at 1550 °C, the strong characteristic diffraction peaks of TiC and SiO₂ appear at the same time, indicating that TiC is synthesised in the SiC–TiC composite powder. In comparison with the peaks shown in Figure 2c and in addition to the sharp peak-shaped TiC diffraction peak presented in Figure 3c, strong SiC diffraction peaks appear in the synthesised product when the holding time at 1550 °C is 2 h. At the same time, the characteristic diffraction peak of SiO₂ disappears, while the other impurity peaks are not yet obvious, indicating that TiC and SiC are completely synthesised. Therefore, as the amount of starch in the system increases, the amount of elemental carbon produced by the decomposition of the starch at high temperatures also increases, thereby remarkably increasing the contact area between the SiO₂ and C particles during the high-temperature synthesis. Furthermore, the formation of SiC between the raw materials of the reactants accelerates. The holding time is extended to 3 h, and the diffraction peaks in the synthesised product do not change significantly. According to the review, a SiC–TiC composite powder is completely produced at 1550 °C for 2 h when the amount of excess starch is 10 wt. %.

Figure 4 shows the XRD patterns of the precursor powder dried at 80 °C and the powder calcined at

1550 °C for different periods with 15 wt. % excess of starch. In comparison with the peaks shown in Figures 2 and 3, a strong TiC characteristic diffraction peak and a weak SiC characteristic diffraction peak are presented in Figure 4b, but no SiO₂ diffraction peak is found. Therefore, as the amount of starch in the system further increases, the amount of elemental carbon generated at high temperatures increases; consequently, the contact area between the SiO₂ and C particles increases during high-temperature synthesis, and the reaction time for the SiC formation shortens. The following analysis of the mass loss also indicates that the SiC–TiC composite powder is relatively synthesised completely at 1550 °C

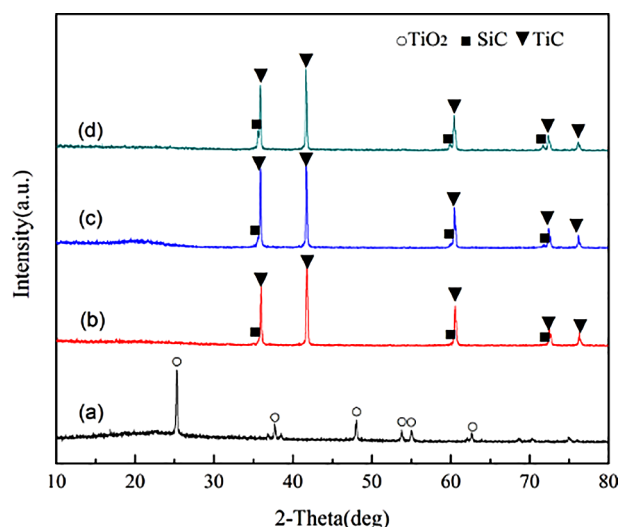


Figure 4. XRD patterns of the samples containing 15 wt. % excess of starch, dried at 80 °C, and maintained at 1550 °C for different periods: a) 80 °C, b) 1550 °C + 1 h, c) 1550 °C + 2 h, d) 1550 °C + 3 h.

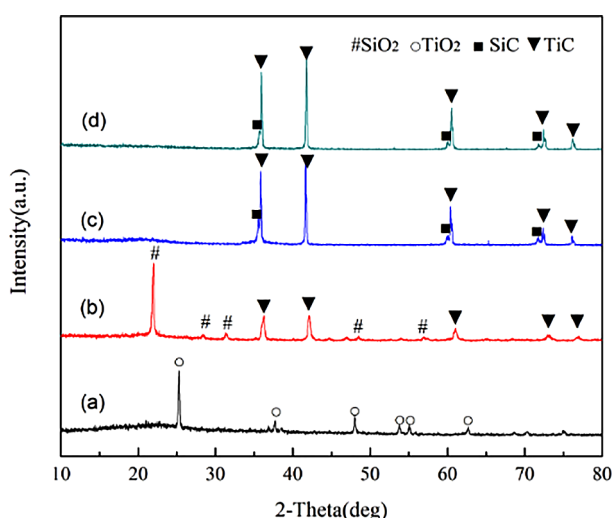


Figure 3. XRD patterns of the samples containing 10 wt. % excess of starch, dried at 80 °C, and maintained at 1550 °C for different periods: a) 80 °C, b) 1550 °C + 1 h, c) 1550 °C + 2 h, d) 1550 °C + 3 h.

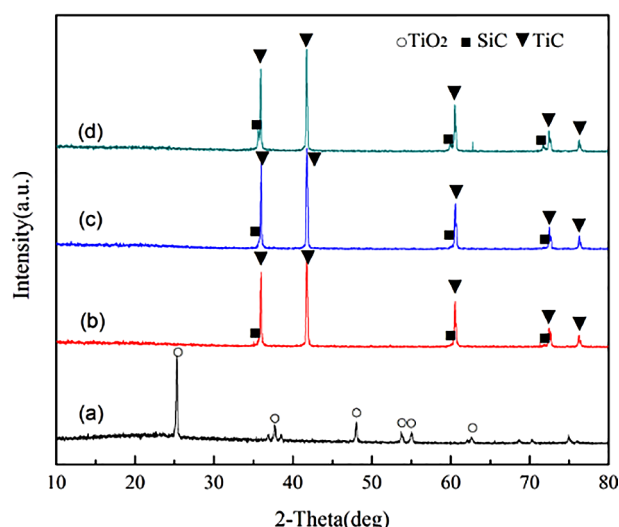


Figure 5. XRD patterns of the samples containing 20 wt. % excess of starch, dried at 80 °C, and maintained at 1550 °C for different periods: a) 80 °C, b) 1550 °C + 1 h, c) 1550 °C + 2 h, d) 1550 °C + 3 h.

for 2 h with 15 wt. % excess of starch. Figure 5 illustrates the XRD patterns of the precursor powder dried at 80 °C and the powder calcined at 1550 °C for different periods with 20 wt. % excess of starch. The XRD patterns of the various phases in Figure 5 exhibit changes similar to those in Figure 4. This result demonstrates that the SiC–TiC composite powders are completely synthesised at 1550 °C for 2 h in the presence of 20 wt. % excess of starch.

Degree of the synthesis reaction

Table 1 shows the mass loss during the synthesis reaction at 1550 °C for different holding times. It can be seen from Table 1 that when the amount of starch is the same, with the extension of the holding time, the mass loss of the synthesis reaction in the system increases, and the reaction process is obviously strengthened. When the amount of excess starch is 5 wt. % and the holding time is 1 h, the mass loss during the reaction is 67.9 %. When the holding time is 2 h, the mass loss during the reaction increases to 80.0 %; when the holding time continues to increase to 3 h, the mass loss only increases by 2.6 %.

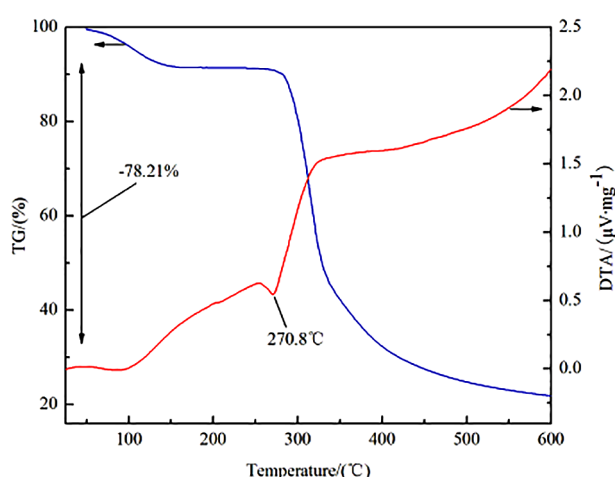


Figure 6. TG-DTA curve of a single starch raw material under an argon atmosphere.

When the amount of excess starch is 10 wt. %, 15 wt. %, and 20 wt. %, the mass loss of synthesis in the system shows similar changes under different holding time conditions. When the holding time is 2 and 3 h, the mass loss of the synthesis in the system is, at most, as high as 80 - 85 wt. %. During the carbothermal reduction to synthesise the SiC–TiC composite powder, the mass loss is higher because of the following: On the one hand, under an argon atmosphere, the TG–DTA curve of a single starch raw material (Figure 6) shows that the starch decomposes, resulting in a mass loss of up to 78.2 %. That is, it decomposes to form elemental carbon and gaseous H₂O at low temperatures. At high temperatures, the starch continuously decomposes to produce a certain amount of gas-phase products, such as CO, CO₂, and C_xH_y, which are discharged with the airflow, resulting in a quality loss [16]. On the other hand, the gaseous SiO as the intermediate product forms and escapes in the carbothermal reduction of SiO₂ and carbon to produce the SiC powder, thereby causing a quality loss [18].

Microstructure

Figure 7 shows the SEM photographs of the precursor powder dried at 80 °C and the powder calcined at 1550 °C for different periods with 10 wt. % excess of starch. In Figure 7a, the dried sample is mainly spherical and massive, and other loose raw material particles are stacked together. The powder samples prepared at 1550 °C for 1 h is mainly composed of a certain amount of coarse flake particles and numerous small irregularly shaped particles; furthermore, agglomeration or adhesion occurs between the powder particles, as shown in Figure 7b. When the powder sample is kept at 1550 °C for 2 h, its morphological characteristics change significantly. In addition to the flake particles and irregularly shaped particles (particle size of about 50 - 100 nm), uniform and slender whiskers form (about 50 - 100 nm in diameter), and an overlap and entanglement exist between the whiskers, as shown in Figure 7c. In Figure 7d, when

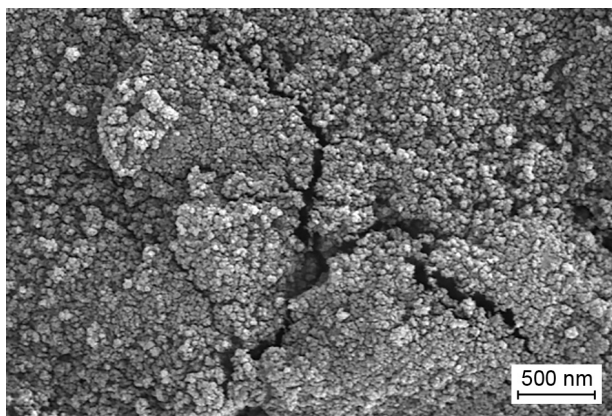
Table 1. Mass loss in the synthesis of SiC–TiC composite powders at 1550 °C for different periods with various amounts of starch

No.	Excess of starch (wt. %)	Holding time (h)	Weight before reaction (g)	Weight after reaction (g)	Mass loss (%)
1	5	1	2.0274	0.6514	67.9
2	5	2	2.0101	0.4017	80.0
3	5	3	2.0134	0.3499	82.6
4	10	1	2.0427	0.6478	68.3
5	10	2	2.0965	0.3886	81.5
6	10	3	2.0256	0.3264	83.9
7	15	1	2.0197	0.6368	68.5
8	15	2	2.0357	0.3528	82.7
9	15	3	2.0009	0.3163	84.2
10	20	1	2.0238	0.6034	70.2
11	20	2	2.0068	0.3279	83.7
12	20	3	2.0114	0.2962	85.3

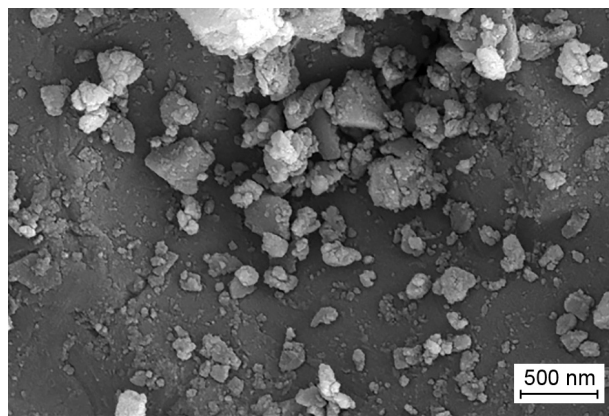
the holding time is 3 h, the whiskers and fine irregularly shaped particles in the synthesised product are greatly reduced, and short rod-shaped and almost flaky coarse particles form. As the holding time increases, the growth of whiskers is inhibited instead.

Figure 8 shows the SEM photographs of the precursor powder dried at 80 °C and the powder calcined

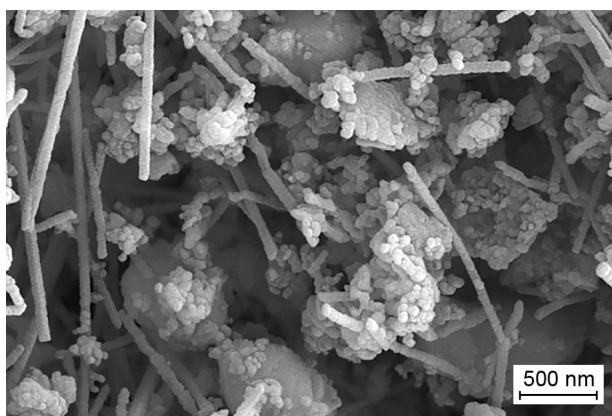
at 1550 °C for different durations with 20 wt. % excess of starch. The morphological characteristics in Figures 8a and 8b are similar to those in Figure 7. The precursor powder samples dried at 80 °C are mainly composed of spherical and massive microstructures with 20 wt. % excess of starch. The powder samples prepared at 1550 °C for 1 h are mainly composed of coarse flaky particles



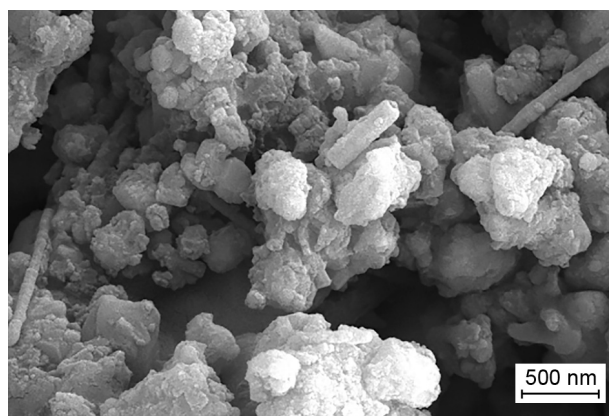
a) 80 °C + 24 h



b) 1550 °C + 1 h



c) 1550 °C + 2 h

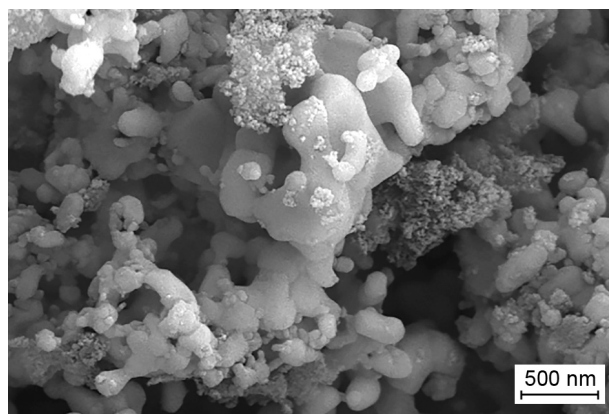


d) 1550 °C + 3 h

Figure 7. SEM photographs of the precursor powder dried at 80 °C and the powder calcined at 1550 °C for different durations with 10 wt. % excess of starch.



a) 80 °C + 24 h



b) 1550 °C + 1 h

Figure 8. SEM photographs of the precursor powder dried at 80 °C and the powder calcined at 1550 °C for different durations with 20 wt. % excess of starch. (Continue on next page)

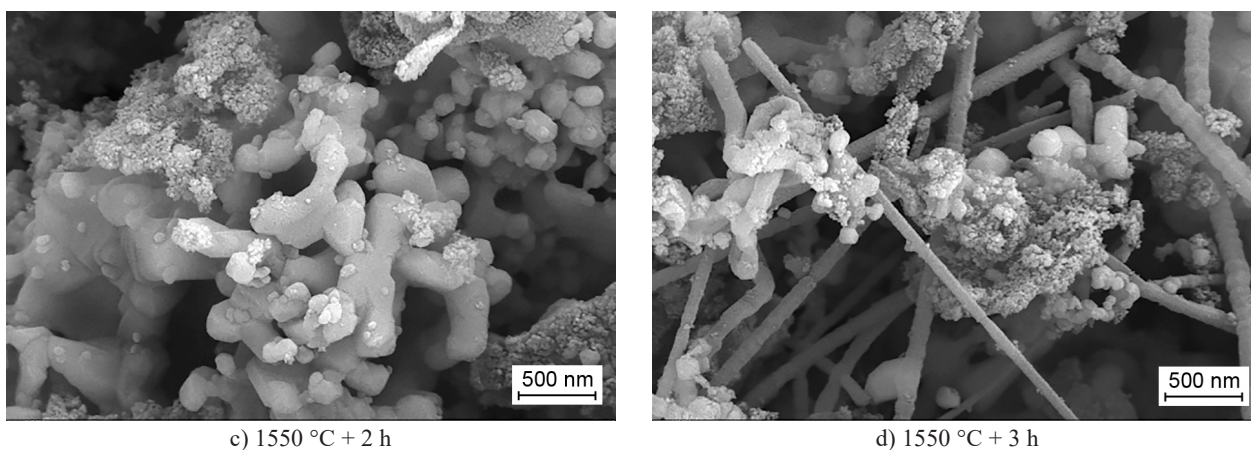


Figure 8. SEM photographs of the precursor powder dried at 80 °C and the powder calcined at 1550 °C for different durations with 20 wt. % excess of starch.

and small irregularly shaped particles. Agglomeration or adhesion exists between the powder particles, as shown in Figure 8b. When the powder samples are kept at 1550 °C for 2 h, their morphological characteristics do not change significantly, as shown in Figure 8c. When the synthesised product is kept at 1550 °C for 3 h, its morphological characteristics change greatly. The prepared powder samples are mainly composed of flake

particles, irregularly shaped particles, and many thin and long whiskers (about 100 - 200 nm in diameter) with different thicknesses. A certain amount of overlap and entanglement occur between the whiskers, as shown in Figure 8d.

Figure 9 shows the SEM photographs of the powder samples calcined at 1550 °C for 2 h with 5 wt. %, 10 wt. %, 15 wt. %, and 20 wt. % excess of starch, re-

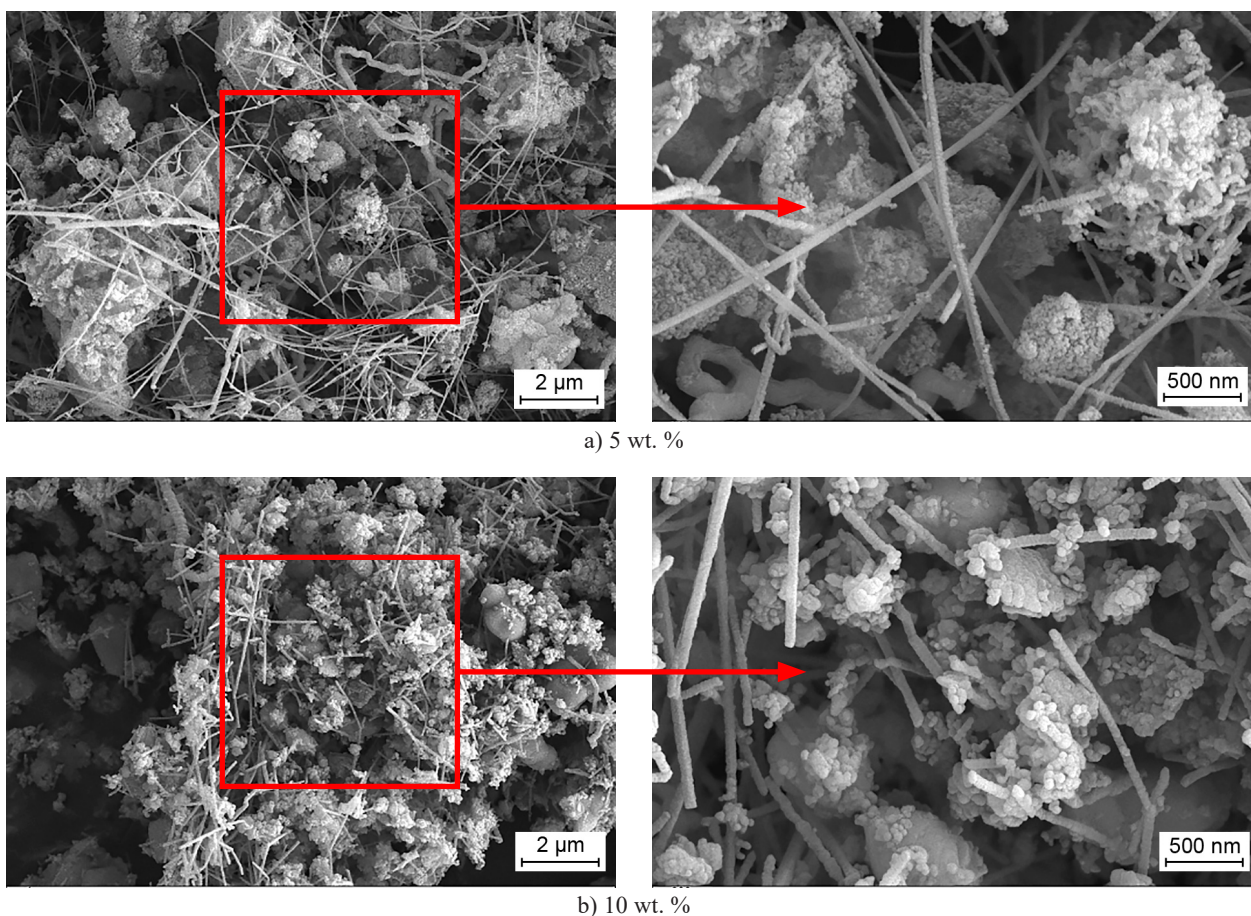


Figure 9. SEM photographs of powder samples calcined at 1550 °C for 2 h with: a) 5 wt. %, b) 10 wt. % excess of starch. (Continue on next page)

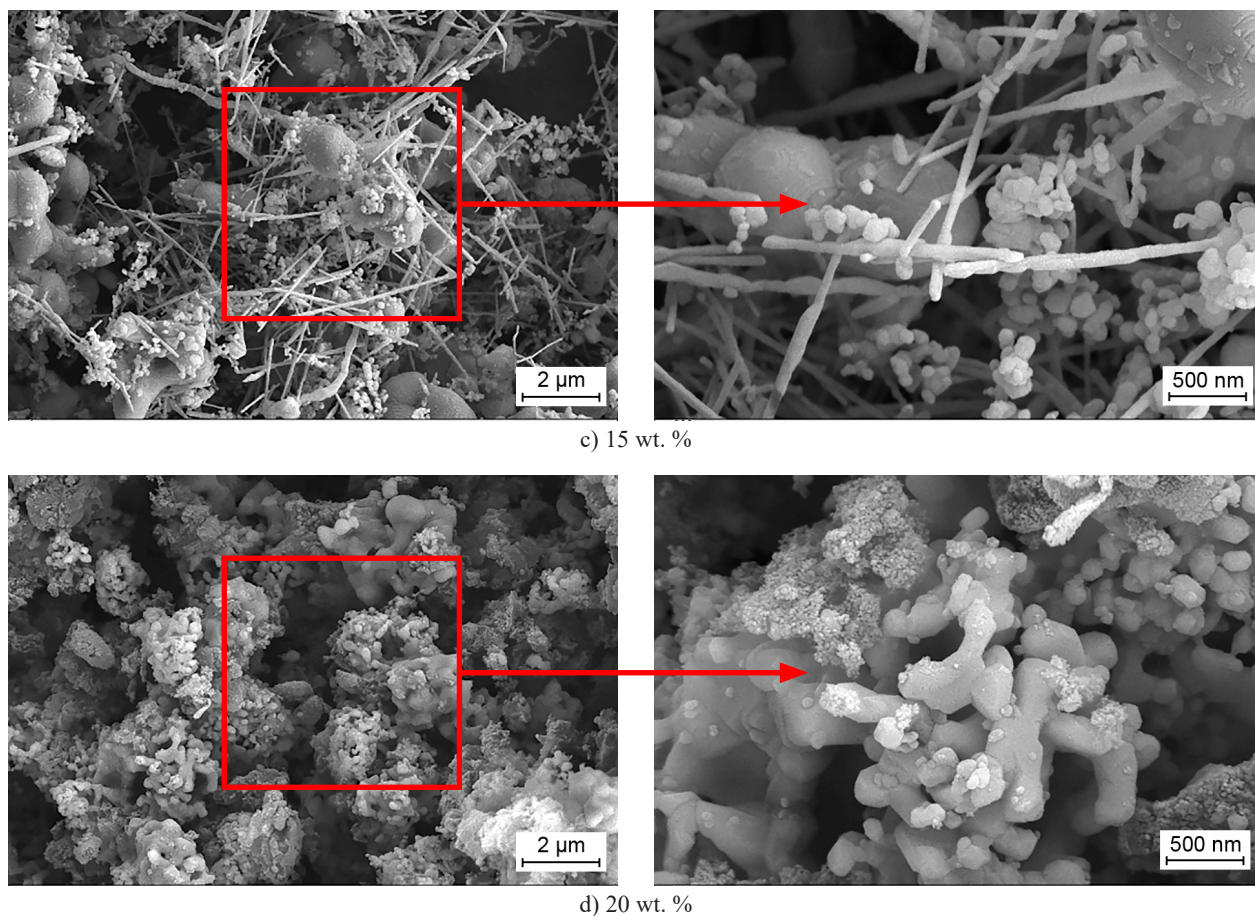


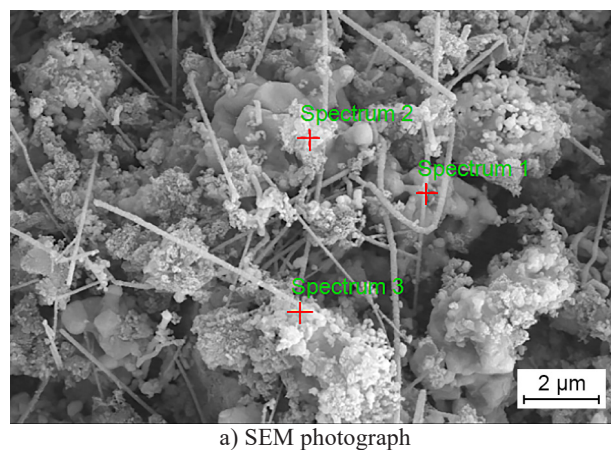
Figure 9. SEM photographs of powder samples calcined at 1550 °C for 2 h with: c) 15 wt. %, d) 20 wt. % excess of starch.

spectively. In comparison with the findings in Figures 9a to 9c, the morphological characteristics of these powder samples with 5 - 15 wt. % excess of starch calcined at 1550 °C for 2 h are mainly composed of flake particles, almost spherical particles, irregularly shaped particles and elongated whiskers, thereby forming a diversified microstructure. However, the morphological characteristics of the powder samples calcined at 1550 °C for 2 h mainly changed when the amount of excess starch is 20 wt. %. The powder samples are mainly composed of flaky coarse particles and approximately spherical fine particles, as shown in Figure 9d.

Energy spectrum analysis

Figure 10 shows the SEM photographs and the EDS analysis results of the powder samples containing 20 wt. % excess of starch synthesised at 1550 °C for 3 h. The synthesised product mainly contains three elements, namely, C, Si, and Ti, indicating that the SiC–TiC composite powders are successfully synthesised in the system under this reaction condition. SiC whiskers are formed via two main mechanisms: gas–liquid–solid (VLS) and gas–solid (VS). In a carbothermal reduction without additives, the formation of SiC whiskers mainly follows the VS mechanism [19]. In the present study, the SiO₂ in the

precursor reacts with C from the starch decomposition at high temperatures to produce SiO and CO; some SiO and C undergo a gas–solid reaction to form SiC particles, and the remaining parts of the SiO and CO undergo a gas–gas reaction to form the crystal nucleus of the SiC; under suitable conditions, the crystal nucleus of the SiC seeks to grow along a specific direction to prepare SiC whiskers [20].



a) SEM photograph

Figure 10. SEM photograph and EDS analysis result of the powder samples with 20 wt. % excess of starch synthesised at 1550 °C for 3 h. (Continue on next page)

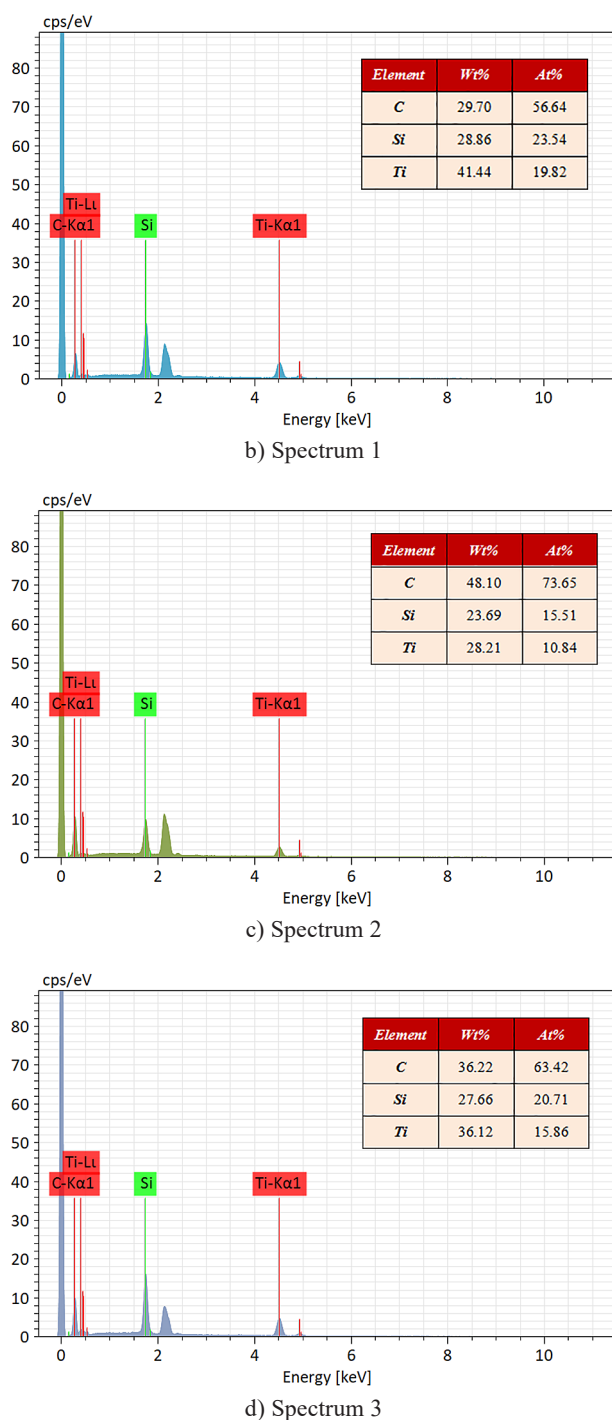


Figure 10. SEM photograph and EDS analysis result of the powder samples with 20 wt. % excess of starch synthesised at 1550 °C for 3 h.

CONCLUSIONS

Both SiO_2 compounds in the silica sol as a raw material and the elemental carbon generated through the decomposition of the raw starch materials at high temperatures mainly exist in a system in their amorphous forms. SiC–TiC composite powders are completely synthesised after holding at 1550 °C for 3 h when the

amount of excess starch is 5 wt. %. Similarly, SiC–TiC composite powders are completely synthesised under the condition of holding at 1550 °C for 2 h when the amount of excess starch is 10 - 20 wt. %. This finding is basically consistent with the analysis result of the mass loss during synthesis.

The morphological characteristics of the powder samples with 5 - 15 wt. % excess of starch calcined at 1550 °C for 2 h mainly include flake particles, spherical particles, irregularly shaped particles and elongated whiskers, forming a diversified microstructure. In comparison, the powder samples calcined at 1550 °C for 2 h are mainly composed of flaky coarse particles and approximately spherical fine particles, but they hardly contain any whiskers.

Acknowledgements

This work is supported by the Key R & D Project in Hunan Province (Grant No. 2021GK2015), the Planned Science and Technology Program of Hunan Province, China (Grant No. 2016TP1028) and the Natural Science Foundation of Hunan Province, China (Grant No. 2016JJ6047).

REFERENCES

- Xu T., Cheng S., Jin L., Zhang K., Zeng T. (2020): High-temperature flexural strength of SiC ceramics prepared by additive manufacturing. *International Journal of Applied Ceramic Technology*, 17(2), 438-448. doi: 10.1111/ijac.13454
- Kim K.J., Lim K.Y., Kim Y.W. (2014): Electrical and thermal properties of SiC ceramics sintered with yttria and nitrides. *Journal of the American Ceramic Society*, 97(9), 2943-2949. doi: 10.1111/jace.13031
- Cornolti L., Martinelli S., Bianchi G., Ortona A. (2019): Microwave heating controlled reactive melt infiltration for graphite-Si–SiC ceramics manufacturing. *Journal of the American Ceramic Society*, 102(5), 2304-2315. doi: 10.1111/jace.16124
- Vajdi M., Moghanlou F.S., Nekahi S., Ahmadi Z., Asl M.S. (2020): Role of graphene nano-platelets on thermal conductivity and microstructure of TiB_2 –SiC ceramics. *Ceramics International*, 46(13), 21775-21783. doi: 10.1016/j.ceramint.2020.05.289
- Yao M., Wang Y., Chen L., Ouyang J., Li H., Gu H., Zhou Y. (2021): Mechanical properties and microstructural evolution of pressureless sintered ceramics obtained from high-energy ball-milled TiB_2 –TiC powders. *Materials Science and Engineering A*, 819(5), 141510-141519. doi: 10.1016/j.msea.2021.141510
- Wang X.C., Zhao J., Cui E.Z., Sun Z.F., Yu H. (2021): Grain growth kinetics and grain refinement mechanism in Al_2O_3 /WC/TiC/graphene ceramic composite. *Journal of the European Ceramic Society*, 41(2), 1391-1398. doi: 10.1016/j.jeurceramsoc.2020.10.019
- Ge D., Deng J., Duan R., Li X., Yue H. (2019): Effect of surface wettability on tribological properties of Al_2O_3 /TiC

- ceramic under wet lubrication. *Ceramics International*, 45(18), 24554–24563. doi: 10.1016/j.ceramint.2019.08.184
8. Asl M.S., Ahmadi Z., Namini A.S., Babapoor A., Motallabzadeh A. (2019): Spark plasma sintering of TiC–SiC_w ceramics. *Ceramics International*, 45(16), 19808–19821. doi: 10.1016/j.ceramint.2019.06.236
 9. Wang F., Xiang D., Wang Y., Li J. (2017): Rapid synthesis of SiC powders by spark plasma-assisted carbothermal reduction reaction. *Ceramics International*, 43(6), 4970–4975. doi: 10.1016/j.ceramint.2017.01.003
 10. Chen X., Fan J., Lu Q. (2018): Synthesis and characterization of TiC nanopowders via sol-gel and subsequent carbothermal reduction process. *Journal of Solid State Chemistry*, 262, 44–52. doi: 10.1016/j.jssc.2018.03.006
 11. Oghenevweta E.J., Wexler D., Calka A. (2016): Early stages of phase formation before the ignition peak during mechanically induced self-propagating reactions (MSRs) of titanium and graphite. *Scripta Materialia*, 122, 93–97. doi: 10.1016/j.scriptamat.2016.05.028
 12. Song M., Yang Y., Xiang M., Zhu Q., Zhao H. (2020): Synthesis of nano-sized TiC powders by designing chemical vapor deposition system in a fluidized bed reactor. *Powder Technology*, 380, 256–264. doi: 10.1016/j.powtec.2020.11.045
 13. Su X., Zhou W., Jie X., Wang J., He X., Chong F., Li Z. (2012): Preparation and dielectric property of Al and N Co-doped SiC powder by combustion synthesis. *Journal of the American Ceramic Society*, 95(4), 1388–1393. doi: 10.1111/j.1551-2916.2011.04996.x
 14. Hu J.L., Xiao H.N., Li Q., Guo W.M., Gao P.Z. (2011): Synthesis and growth mechanism of TiC–SiC composite powders by carbothermal reduction. *The Chinese Journal of Nonferrous Metals*, 21(5), 1131–1136. doi: 10.3354/cr00999
 15. Hu J.L., Peng H.X., Hu C.Y., Guo W.M., Tian X.Y., Peng Y.X. (2017): Effects of different carbon sources and reaction temperatures on the synthesis of SiC–TiC composite powders by carbothermal reduction. *Journal of Ceramic Processing Research*, 18(1), 79–85.
 16. Sun H.Y., Kong X., Sen W., Liu G.Y., Yi Z.Z. (2015): Synthesis and characterization of TiC powders by carbothermal reduction method in vacuum. *Advanced Materials Research*, 1089(1), 147–151. doi:10.4028/www.scientific.net/AMR.1089.147
 17. Hu J.L., Hu C.Y., Guo W.M., Wang X.C., Tian X.Y., Peng Y.X. (2017): Synthesis of SiC–TiC composite powders using glucose as carbon source. *Journal of Synthetic Crystals*, 46(2), 311–315.
 18. Sharma N.K., Williams W.S., Zangvil A. (1984): Formation and structure of silicon carbide whiskers from rice hulls. *Journal of the American Ceramic Society*, 67(11), 715–720. doi: 10.1111/j.1151-2916.1984.tb19507.x
-